

Submitted to JAMES

Community Earth System Model version 2 (CESM2) Special Collection

Characteristics of Future Warmer Base States in CESM2

Gerald A. Meehl¹, Julie M. Arblaster^{1,2}, Susan Bates¹, Jadwiga H. Richter¹, Claudia Tebaldi³,
Andrew Gettelman¹, Brian Medeiros¹, Julio Bacmeister¹, Patricia DeRepentigny⁴,
Nan Rosenbloom¹, Christine Shields¹, Aixue Hu¹, Haiyan Teng¹,
Michael J. Mills¹, and Gary Strand¹

1. National Center for Atmospheric Research, Boulder, CO, ORCID: 0000-0002-8760-9534
2. School of Earth, Atmosphere and Environment, Monash University, Melbourne, Australia
3. PNNL, Washington, D.C.
4. Department of Atmospheric and Oceanic Sciences and Institute of Arctic and Alpine Research, University of Colorado, Boulder, Colorado, USA.

December 30, 2019

Key Points:

- Two versions of the Community Earth System Model version 2 (CESM2(CAM6), and CESM2(WACCM6)) have higher equilibrium climate sensitivity (ECS) but about the same transient climate response (TCR) compared to the previous version (CESM1)
- The latest generation of the Whole Atmosphere Community Climate Model (WACCM6) high top comprehensive chemistry atmospheric model coupled to the same earth system components as CESM2(CAM6), becoming CESM2(WACCM6), has about the same TCR but lower ECS compared to CESM2(CAM6)
- Future warming among model versions and scenarios diverges around 2050, with greater warming by end of century in the higher forcing scenarios and in both versions of CESM2 with higher ECS compared to CESM1
- There is more future warming (and greater precipitation increase) in the tropics in the CESM2 versions compared to CESM1,
- There is less future warming in the tropical Pacific in CESM2(CAM6) compared to CESM2(WACCM6) with correspondingly less precipitation increase

Keywords: Community Earth System Model (CESM); Global coupled Earth system modeling;

Future climate projections; Emission scenarios

Plain Language Summary

The new earth system model versions CESM2(CAM6) and CESM2(WACCM6) have higher equilibrium climate sensitivity than the previous model version CESM1. While this higher climate sensitivity produces greater warming by the end of the 21st century in CESM2(CAM6) and CESM2(WACCM6) compared to CESM1 for the high forcing scenario, prior to mid-century the warming is comparable among all model versions and scenarios. The higher climate sensitivity in CESM2(CAM6) and CESM2(WACCM6) compared to CESM1 produces greater tropical warming and precipitation increases in those regions. CESM2(CAM6) does not warm as much in the tropics as CESM2(WACCM6), though CESM2(CAM6) shows an ice-free Arctic in September for all scenarios and ensemble members about a decade earlier than in CESM2(WACCM6).

Abstract

Simulations of 21st century climate with Community Earth System Model version 2 (CESM2) using the standard atmosphere (CAM6), denoted CESM2(CAM6), and the latest generation of the Whole Atmosphere Community Climate Model (WACCM6), denoted CESM2(WACCM6), are presented, and a survey of general results is described. The equilibrium climate sensitivity (ECS) of CESM2(CAM6) is 5.3°C, and CESM2(WACCM6) is 4.8°C, while the transient climate response (TCR) is 2.1°C in CESM2(CAM6) and 2.0°C in CESM2(WACCM6). Thus, these two CESM2 model versions have higher values of ECS than the previous generation of model, the CESM(CAM5) (hereafter CESM1), that had an ECS of 4.1°C, while the CESM1 value of TCR was 2.3°C. Though the previous generation Representative Concentration

Pathways (RCPs) and current generation Shared Socioeconomic Pathways (SSPs) have somewhat different forcings, these higher sensitivities are reflected in higher values of global surface temperature increase by 2100 in CESM2(CAM6) and CESM2(WACCM6) compared to CESM1 between comparable emission scenarios for the high forcing scenario. This amounts to about 1°C greater warming for SSP5-8.5 compared to CESM1 by the end of the 21st century, but nearly the same warming for all model versions at year 2100 for the two lower forcing scenarios, SSP2-4.5 and SSP1-2.6. Future warming among CESM2 model versions and scenarios diverges around 2050 such that the higher values of ECS and TCR in CESM2(CAM6) and CESM2(WACCM6) do not appreciably produce greater warming before mid-century than in the previous version of CESM1 with lower ECS. The larger values of TCR and ECS in CESM2(CAM6) compared to CESM1 are manifested by greater warming in the tropics. CESM2(CAM6) shows less warming in the tropical Pacific than CESM2(WACCM6) and comparatively less future precipitation increase. Associated with a higher climate sensitivity, for CESM2(CAM6) an ice-free Arctic in September occurs for all scenarios and ensemble members in the 2030-2050 time frame, but about a decade later in CESM2(WACCM6), occurring around 2040-2060.

1. Introduction

A number of versions of the Community Earth System Model version 1 (CESM1) were described by Hurrell et al (2013, CESM1), Kay et al (2015, CESM1.1, the large ensemble), and Meehl et al. (2019a, CESM1.3). Here we describe future climate characteristics of a new

generation of the CESM, the CESM2. As presented in the general model description with abundant details (Danabasoglu et al., 2019), the new model versions here are “CESM2(CAM6)” (Community Atmosphere Model Version 6, CAM6) and “CESM2(WACCM6)” (Whole Atmosphere Community Climate Model Version 6, WACCM6). The latter is more fully described by Gettelman et al. (2019a) and is the high-top version to accompany the low-top CESM2(CAM6), but both use the same ocean, land, and sea ice components, as well as the same tropospheric atmospheric physics (with a few differences, see discussion below) and dynamical core. To provide context for the future warmer base states in the different scenario simulations, we will review general climate sensitivity metrics, the ECS (derived from the “Gregory method” (Gregory, et al., 2004) from an instantaneous 4xCO₂ simulation), and the TCR (the global average surface warming in a 1% per year CO₂ increase experiment at the time of CO₂ doubling around year 70). We also will show how CESM1 and CESM2 produce somewhat different patterns of surface temperature and precipitation change in a future warmer climate, differences between the responses of CESM2(CAM5) and CESM2(WACCM6), as well as how sea ice changes in the Arctic and Antarctic in the future warmer base states in the model versions. The intention here is to provide a survey of general model response characteristics and point to other studies in the CESM2 virtual special issue that explore various features in more detail.

2. Model characteristics

There have been a number of changes implemented in CESM2 compared to previous versions of CESM1 noted above. These are described in detail in Danabasoglu et al., (2019) and briefly summarized here. The CESM2 uses a nominal 1° (1.25° in longitude and 0.95° in latitude)

horizontal resolution configuration with 32 vertical levels and a model top at 3.6 hPa (about 40 km, termed “low top”) with a finite volume dynamical core and limited chemistry. In the atmosphere, the separate representations of the boundary layer, shallow convection and large-scale condensation (e.g. the boundary layer in the University of Washington, UW, scheme and Park scheme for shallow convection and macrophysics in CESM1) have been replaced by the Clouds Unified By Binormals parameterization (CLUBB, Golaz et al., 2002). CLUBB is a high order turbulence closure scheme, and uses simple PDFs to describe the sub-grid scale distributions of key humidity, saturation, temperature and vertical velocity quantities. The previous version of the Morrison Gettleman (MG1) microphysics scheme in CESM1 has been updated to MG2 in CESM2. The MG2 scheme now predicts rather than diagnoses precipitating hydrometeors (Gettelman and Morrison, 2015), and links mixed phase ice nucleation to aerosols, rather than just temperature as in CESM1. Direct modifications to the Zhang-McFarlane deep convection scheme (Neale et al., 2008; Zhang and McFarlane, 1995) act to further increase humidity sensitivity, and the near-surface stress scheme of Beljaars et al. (2004) acts to reduce excessive drag seen in CESM1. The final major change was to advance the modal aerosol scheme from 3 to 4 modes (MAM4, Liu et al., 2016) including an improved aging process for black carbon.

The ocean model in CESM2 is a version of POP used in CESM1 but with many improvements to the physics (Danabasoglu et al., 2019). It has a nominal 1° horizontal resolution and enhanced resolution in the equatorial tropics, and 60 levels in the vertical. Other features of CESM2 involving land and sea ice are described in detail by Danabasoglu et al., (2019).

WACCM6 is a “high top” chemistry and climate model with 70 levels in the vertical which extend up to ~140 km in the upper atmosphere, coupling the same nominal 1° latitude-longitude grid spacing in the atmosphere and ocean to form CESM2(WACCM6) as in CESM2(CAM6). WACCM6 simulations differ from CAM6 simulations only in (a) the higher vertical lid, (b) full stratospheric and tropospheric chemistry instead of fixed oxidants in CAM6, and (c) additional non-orographic gravity wave drag parameterization in WACCM6. The other coupled components (ocean, sea ice, land) are identical in CESM2(WACCM6) and CESM2(CAM6). Full details of the WACCM6 configuration are described in Gettelman et al., 2019a.

Here we show results for 21st century simulations with four future emission scenarios (SSP1-2.6, SSP2-4.5, SSP3-7.0, and SSP5-8.5, see O’Neill et al., 2016, for descriptions) for CESM2(CAM6) and CESM2(WACCM6). We use all available ensemble members, from e.g. one for SSP1-2.6 for CESM2(WACCM6) and up to ten for SSP3-7.0 for CESM2(CAM6) (see Table 1), and three for the previously-documented RCP scenarios for CESM1. Statistical significance is assessed via a t-test, taking into account the varying number of members in each ensemble. For differences between the model versions, we use non-overlapping 20 year averages from the multi-century PIcontrol simulations as a measure of the variance.

The ECS, calculated with the standard “Gregory method” as noted above (Gregory et al., 2004), of CESM2(CAM6) is 5.3°C, and that of CESM2(WACCM6) is 4.8°C, while the TCR of 2.1°C in CESM2 and 2.0°C in WACCM6. Here, TCR is calculated as the difference between the year 61-80 average in a 1% CO₂ increase experiment (where CO₂ doubles around year 70) minus the linear fit to the piControl runs for the 150 years concurrent to those in the 1% CO₂ runs. A

variation in the TCR calculation for the control run reference period, for example in the ESMVal Tool, uses a linear fit of the piControl run for all 140 years of the 1% CO₂ experiment prior to the TCR calculation. Yet another variant is to form the difference relative to the comparable years 61-80 in the piControl run (as in Meehl et al., 2013, with the cited value here for CESM1 from that paper). Differences in TCR between these various methods are slight, usually only on the order of $\sim 0.1^{\circ}\text{C}$.

There also are a number of variations in how ECS is calculated, and one alternative uses the atmospheric models coupled to a non-dynamic slab ocean, which yields ECS values for CESM2(CAM6) of 5.3°C , and CESM2(WACCM6) of 5.1°C (Danabasoglu et al., 2019). A more detailed exploration of ECS methodologies and issues involved with them is given in Bacmeister et al. (2019). In any case, these CESM2 model versions have higher values of ECS than the previous generation of model, the CESM1, which has an ECS of 4.1°C calculated by the standard Gregory method, with a TCR of 2.3°C (Meehl et al., 2013). The higher values of ECS in the two CESM2 versions are due to cloud feedbacks (Gettelman et al 2019b). Specifically, changes made to increase high latitude supercooled liquid water, and to adjust warm rain susceptibility to aerosols in shallow clouds have increased cloud feedbacks (Gettelman et al 2019b). A more extensive documentation of features involved with ECS and TCR in the CESM2 is given in Bacmeister et al. (2019). The latest ECS values from both CESM2 versions are in the upper end of the CMIP6 ECS and TCR ranges of 1.9°C - 5.6°C , while the TCR values are more in the middle of the CMIP6 range of 1.6°C - 3.0°C (Table 2, and Meehl et al., 2019b).

Possible reasons for the relationship between ECS and TCR values are reviewed by Meehl et al. (2019b) and described by references therein.

Table 1: Number of ensemble members for the future scenario runs to 2100 for CESM2(CAM6) and CESM2(WACCM6) (* = only 1 member with output post-2055). Three members are used for CESM1.

Model	SSP1-2.6	SSP2-4.5	SSP3-7.0	SSP5-8.5
CESM2(CAM6)	2	3	10	3
CESM2(WACCM6)	1	2	3*	2

Table 2. ECS and TCR values for CESM2(CAM6), CESM2(WACCM6), and CESM1 (°C); methods for calculating these values are discussed in the text.

Model	ECS	TCR
CESM2	5.3°C	2.1°C
WACCM6	4.6°C	2.0°C
CESM1	4.1°C	2.3°C

3. Globally averaged temperature response

Though the Representative Concentration Pathway (RCP) and Shared Socioeconomic Pathway (SSP) emission scenarios have somewhat different forcings, the experimental design of ScenarioMIP (O'Neill et al., 2016) deliberately chose a number of concentration pathways that could provide continuity with CMIP5, and therefore allow comparison of outcomes between generation of models (SSP1-2.6, SSP2-4.5 and SSP5-8.5 in ScenarioMIP Tier 1 should be directly comparable to RCP2.6, RCP4.5 and RCP8.5, aiming at achieving the same radiative forcings by 2100). Further, Forster et al. (2019) indicate that the temperature responses are comparable in the two sets of scenarios. The higher climate sensitivity in the CESM2 versions is reflected in higher values of global surface temperature increase by 2100 between comparable emission scenarios only for the higher forcing scenario (Fig. 1). The CESM2 versions have about 1°C greater warming for SSP5-8.5, but nearly the same warming at 2100 for the two lower forcing scenarios, SSP2-4.5 and SSP1-2.6. Before about the mid-21st century, the warming in all model versions and scenarios is nearly indistinguishable. This is consistent with previous results that have demonstrated that the response to different emission scenarios does not diverge until about mid-century (O'Neill et al., 2016). It also appears that model versions with higher ECS over the next several decades do not produce appreciably greater warming. This is consistent with our understanding of the timescales at which TCR and ECS are relevant, with TCR more representative of the response over the next 50 years or so (Fig. 1b shows nearly the same temperature response in the 1% CO₂ increase runs until around the time of CO₂ doubling near year 70), and ECS for higher forcing at longer timescales (note divergence of response in the 1% CO₂ increase runs in Fig. 1b as the models approach 150 years where CO₂ is nearly quadrupled; see also Meehl et al. 2019b and references therein). A different response to non-CO₂ forcings

(e.g. aerosols) between the CESM1 and CESM2 versions could also potentially contribute to the divergence between them in the latter decades of the 21st Century.

To illustrate these points more quantitatively, Fig 2 shows globally averaged temperature differences for the different scenarios, models, and time periods taken from Fig. 1. For the near-term averaged from 2015-2035 (Fig. 2a), as noted above all models and scenarios are virtually indistinguishable, all with warming values around $+0.6^{\circ} \pm 0.1^{\circ}\text{C}$ (uncertainty is the range of responses). Approaching mid-century for the time period 2031-2050 (Fig. 2b), all models with the high forcing scenario SSP5-8.5, with warming values of about $+1.4^{\circ} \pm 0.1^{\circ}\text{C}$, can now be distinguished from the other scenarios which cluster around $+1.0 \pm 0.2^{\circ}\text{C}$. After mid-century for the time period 2051-2070 (Fig. 2c), there is greater spread across the models and scenarios. For the low forcing scenarios (SSP1-2.6), CESM1 is about 0.1° - 0.2°C lower than the two CESM2 versions, with warming values for the latter of about 1.4°C . For SSP2-4.5 the different model versions are more comparable, but for SSP3-7.0 there is greater spread between the CESM2 versions and CESM1, likely due to the larger radiative forcing in RCP6.0 compared to SSP3-7.0. Both CESM2 model versions show warming around about $+1.8^{\circ}\text{C}$, while CESM1 is lower with a value of about 1.5°C which is about 0.1°C lower than its value for the lower SSP2-4.5. Meanwhile, for the high forcing scenario SSP5-8.5, both CESM2 models lie near $+2.5^{\circ}\text{C}$ with CESM1 only slightly lower at $+2.4^{\circ}\text{C}$.

For the late century period 2081-2100, there is a clear differentiation between the models and scenarios. It is only for this late-century period that CESM1 with the lower ECS has consistently lower warming values compared to the two CESM2 versions, with the difference in response

being larger for the high amplitude forcing scenario. Though CESM2(WACCM6) has a somewhat lower ECS, there is no appreciable differentiation in the response for this time period compared to CESM2(CAM6), with warming values for the four scenarios of about +1.4°C, +2.4°C, +3.4°C, and +4.8°C, respectively. CESM1 has values lower than those just listed of -0.1°C, -0.2°C, -0.9°C (again likely due to the lower radiative forcing in RCP6.0 compared to SSP3-7.0), and -0.9°C, respectively.

3. Geographical patterns of response

a. Surface air temperature

Surface air temperature anomalies for the four scenarios and two time periods, one near-term and the other end of century, for CESM2(CAM6) and CESM2(WACCM6) are shown in Figs. 3 and 4, respectively. As seen before in previous versions of CESM (e.g. Meehl et al. 2013) and in the CMIP5 models (e.g. Collins et al 2013), there is significant warming almost everywhere in all scenarios in both models and both time periods except for an area of significant cooling in the North Atlantic in association to the weakening of the Atlantic Meridional Overturning Circulation in response to the increased greenhouse gas forcing (e.g., Hu et al., 2013). Warming is generally greater over land areas than ocean, and at high northern latitudes. Somewhat greater warming compared to other ocean areas begins to emerge in the eastern tropical Pacific becoming especially notable in late century in SSP5-8.5 (Figs. 3h, 4h).

Comparing the patterns of CESM2(CAM6) surface temperature response to CESM1 as differences in the anomalies (Fig. 5), the tropics in general are notably warmer (e.g. positive

anomalies of over $+1^{\circ}\text{C}$ in the higher scenarios and late century) while the Arctic appears colder in CESM2(CAM6) (negative differences). These are differences in anomalies as noted above, and CESM2(CAM6) actually starts with a warmer baseline compared to CESM1 (DeRepentigny et al., 2019). The warmer tropics in CESM2 compared to CESM1 was noted to have been present in the 20th century historical simulations and is discussed by Danabasoglu et al (2019). There are some indications that sea ice retreat in CESM2(CAM6) is faster than CESM1 (discussed later in Fig. 11) associated with the warmer baseline Arctic temperatures documented by DeRepentigny et al., (2019) even though there are negative differences in the response of Arctic temperatures in Fig. 6. This indicates in relative terms that CESM2(CAM6) warms less at high latitudes. This is consistent with the TCR being similar in the two model versions, and with the mechanism for higher ECS that involves better representation of high latitude cloudiness in CESM2(CAM6) as noted earlier. This comes with removal of a negative cloud phase feedback (Gettelman et al 2019b), but this is not realized if the high latitude oceans do not warm (Fig 5). Note that CESM2(CAM6) and especially CESM2(WACCM6) has improved Arctic surface fluxes due to increased supercooled liquid water in CESM2(CAM6) and CESM2(WACCM6) improves upon this with a better distribution of aerosols (DuVivier et al., 2019; Gettelman et al., 2019b).

Some interesting features of the responses in the two CESM2 versions emerge when the differences are computed, CESM2(CAM6) minus CESM2(WACCM6) in Fig. 6. For SSP1-2.6 (Figs. 6a,b), CESM2(CAM6) has areas of less warming over northern North America and northwest Asia, as well as the Southern Ocean, the latter being particularly notable for late century (Fig. 6b). Only the latter is noticeable for SSP2-4.5 and in late century (Fig. 5d). Meanwhile in the tropical Pacific and to a lesser extent in the tropical Atlantic, negative

differences indicate there is a tendency for less warming in CESM2(CAM6) compared to CESM2(WACCM6).

b. Precipitation

Previous CESM model versions (e.g. Meehl et al., 2013) and the CMIP5 models (e.g. Collins et al 2013) have shown that a warmer climate generally produces greater tropical precipitation, reduced precipitation in the subtropics, and increases at mid- and high latitudes where warmer air has an increased capacity for moisture. This pattern is seen for all scenarios and both time periods in both the CESM2(CAM6) and CESM2(WACCM6) (Figs. 7 and 8).

For the comparison between CESM1 and CESM2(CAM6) (Fig. 9), as could be expected from the discussion above, the CESM2(CAM6) with the warmer tropics produces greater tropical precipitation (positive anomalies) compared to CESM1 in all scenarios and time periods. The expanded Hadley Circulation noted in previous studies (e.g. Kang et al., 2013), associated with those positive tropical precipitation anomalies, is associated with mainly reductions in subtropical precipitation in CESM2(CAM6) compared to CESM1 (negative anomalies in Fig. 9 in those regions) for all scenarios and time periods.

For the differences between the CESM2(CAM6) and CESM2(WACCM6), those generally relate to the surface temperature differences, with the CESM2(CAM6) with its cooler tropical Pacific producing reduced precipitation there, and the other tropical oceans responding in part to locally warmer SSTs and partly to the likely effects of a weakened Walker circulation to produce positive precipitation anomalies as evident in all scenarios and both time periods (Fig. 10). The

response in the subtropics is sometimes connected to regional SSTs, with areas of increased SSTs and precipitation in CESM2(CAM6) (e.g. Australia and southeastern Indian Ocean in SSP5-8.5, Fig. 10g,h), while other areas have likely more to do with other regional or remote forcing (e.g. subtropical Atlantic and South Asia in SSP2-4.5, Fig. 10c,d). The role of changes in the Hadley Circulation related to these patterns of precipitation change will be the subject of a subsequent paper.

4. Sea Ice

A detailed discussion of future sea ice response in CESM2(CAM6) and CESM2(WACCM6) is given in DuVivier et al (2019) and DeRepentigny et al. (2019) and we mention only a few aspects here for context. In general for Arctic (Fig. 11) and Antarctic (Fig. 12) sea ice, both CESM2(CAM6) and CESM2(WACCM6) simulate less sea ice extent than CESM1, with CESM2(WACCM6) being in better agreement with the observations (discussed in greater detail in DuVivier et al., 2019). Also the timing of an ice-free Arctic in September (defined as ice extent falling below 1 million km², indicated by the dashed line in Fig. 11) occurs roughly ten years earlier for all scenarios in CESM2(CAM6) compared to CESM2(WACCM6), though there is overlap with the CESM1 represented here by the CESM1 large ensemble (Kay et al., 2015; DeRepentigny et al., 2019). There is no scenario dependence on the timing of first ice-free conditions in the Arctic in CESM2(CAM6), but winter ice extent is still very sensitive to the choice of future forcing scenario (Fig. 11, DeRepentigny et al., 2019). In the Antarctic, the CESM2(CAM6) is more in line with observations during the austral summer (Fig. 12a,b) whereas the CESM1 is in closer agreement with observations in the austral winter (Fig. 12c,d).

Note however that neither the CESM2(CAM6) nor the CESM1 is able to reproduce the trend in Antarctic ice extent over the satellite era.

DuVivier et al. (2019) analyze the pre-industrial control and 20th century historical simulations from the two new models, and find that there are fewer aerosols to form cloud condensation nuclei in CESM2(CAM6) compared to CESM2(WACCM6), which results in thinner liquid clouds. This results in more shortwave radiation early in the melt season, driving a stronger ice-albedo feedback and leading to additional sea ice loss and significantly thinner ice year-round. There is the possibility that this stronger ice-albedo feedback in CESM2(CAM6) could contribute to its higher ECS compared to CESM2(WACCM6). These sea ice changes also likely contribute to warmer Arctic conditions in CESM2(CAM6) compared to CESM2(WACCM6) seen most clearly in the higher forcing scenarios (Fig. 6e-h).

5. Conclusions

The new versions of CESM2(CAM6) and CESM2(WACCM6) have higher equilibrium climate sensitivities than the previous model version, CESM1, but comparable values of transient climate response. While this higher climate sensitivity in the newer versions produces greater warming by the end of the 21st century in CESM2(CAM6) and CESM2(WACCM6) compared to CESM1 for the high forcing scenario, prior to mid-century the warming is comparable among all model versions and scenarios. This is consistent with the mechanism for the higher ECS, which is partly related to high latitude cloud feedbacks, and do not take effect until the high latitude oceans warm significantly. The higher climate sensitivity in CESM2(CAM6) and CESM2(WACCM6) compared to CESM1 is associated with greater tropical warming and

precipitation increase in those regions. CESM2(CAM6) does not warm as much in the tropics as CESM2(WACCM6), though CESM2(CAM6) warms more at high latitudes than CESM2(WACCM6). CESM2(CAM6) shows an ice-free Arctic in September for all scenarios and ensemble members about a decade earlier than CESM2(WACCM6) likely due to different representations of Arctic clouds driven by interactive aerosol chemistry. Thus 21st century scenarios are consistent broadly with TCR and ECS estimates, with a significant difference in global average surface temperature in 2100 in CESM2(CAM6) over CESM1 only for the highest forcing scenario. This goes along with the high latitude ice and cloud feedback processes that are responsible for ECS differences between CESM1, CESM2(CAM6) and CESM2(WACCM6).

Model and Data Availability

Previous and current CESM versions are freely available at www.cesm.ucar.edu/models/cesm2/. The CESM solutions / datasets used in this study are also freely available from the Earth System Grid Federation (ESGF) at esgf-node.llnl.gov/search/cmip6 or from the NCAR Digital Asset Services Hub (DASH) at data.ucar.edu or from the links provided from the CESM web site at www.cesm.ucar.edu.

Arctic and Antarctic sea ice extent data are available from:

<http://nsidc.org/data/search/#keywords=Arctic+sea+ice+extent/sortKeys=score,,desc/facetFilters=%257B%257D/pageNumber=1/itemsPerPage=25>

and

<http://nsidc.org/data/search/#keywords=Antarctic+sea+ice+extent/sortKeys=score,,desc/facetFilters=%257B%257D/pageNumber=1/itemsPerPage=25>, respectively.

Acknowledgements

The CESM project is supported primarily by the National Science Foundation (NSF). This material is based upon work supported by the National Center for Atmospheric Research (NCAR), which is a major facility sponsored by the NSF under Cooperative Agreement No. 1852977. Computing and data storage resources, including the Cheyenne supercomputer, were used for the CESM simulations (doi:10.5065/D6RX99HX). This research also used resources of the National Energy Research Scientific Computing Center, a DOE Office of Science User Facility supported by the Office of Science of the U.S. Department of Energy under Contract No. DE-AC02-05CH11231. Portions of this study were supported by the Regional and Global Model Analysis (RGMA) component of the Earth and Environmental System Modeling Program of the U.S. Department of Energy's Office of Biological & Environmental Research (BER) via National Science Foundation IA 1947282.

References

Bacmeister, J., et al., (2019). Abrupt 4xCO₂ increase experiments using the Community Earth System Model (CESM): Relationship to climate sensitivity and comparison of CESM1 to CESM2. *JAMES*, submitted.

Beljaars, A. C. M., Brown, A..R., & Wood, N. (2004). A new parametrization of turbulent orographic form drag. *Quarterly Journal of the Royal Meteorological Society*, *130*, 1327–1347, doi:10.1256/qj.03.73.

Bogenschutz, P. A., Gettelman, A., Hannay, C., Larson, V.E., Neale, R.B., Craig, C., & Chen, C.-C. (2018). The Path to CAM6: Coupled Simulations with CAM5.4 and CAM5.5. *Geosci. Mod. Dev.*, *11*, 235–255, doi:10.5194/gmd-2017-129.

Collins, M. et al. (2013). Long-term Climate Change: Projections, Commitments and Irreversibility. In: *Climate Change 2013: The Physical Science Basis. Contribution of Working Group I to the Fifth Assessment Report of the Intergovernmental Panel on Climate Change*.

Stocker, T.F., D. Qin, G.-K. Plattner, M. Tignor, S.K. Allen, J. Boschung, A. Nauels, Y. Xia, V. Bex and P.M. Midgley (eds.). Cambridge University Press, Cambridge, United Kingdom and New York, NY, USA, doi:10.1017/CBO9781107415324.023.

Danabasoglu, G., et al. (2019). The Community Earth System Model version 2 (CESM2), *JAMES*, submitted.

Dee, D.P., et al. (2011), The ERA-Interim reanalysis: configuration and performance of the data assimilation system. *Q.J.R. Meteorol. Soc.*, 137: 553-597. doi:10.1002/qj.828.

DeRepentigny, P., Jahn, A., Holland, M.M., & Smith, A. (2019). Arctic Sea Ice in the Community Earth System Model Version 2 (CESM2) over the 20th and 21st Centuries, *J. Geophys. Res.--Oceans*, submitted.

DuVivier, A.K., Holland, M.M., Kay, J.E., Tilmes, S., Gettelman, A., & Bailey, D.A., (2019). Arctic and Antarctic sea ice state in the Community Earth System Model Version 2. *J. Geophys. Res.--Oceans*, submitted.

Forster, P.M., Maycock, A.C., McKenna, C.M., & Smith, C.J. (2019). Latest climate models confirm need for urgent mitigation. *Nat. Clim. Change*, <https://doi.org/10.1038/s41558-019-0660-0>.

Gettelman, A., & Morrison, H. (2015). Advanced two-moment bulk microphysics for global models. Part I: Off-line tests and comparison with other schemes. *J. Climate*, 28, 1268–1287, <https://doi.org/10.1175/JCLI-D-14-00102.1>.

Gettelman, A., et al. (2019a). The Whole Atmosphere Community Climate Model 2 Version 6 (WACCM6). *J. Geophys. Res.*, <https://doi.org/10.1029/2019JD030943>.

Gettelman, A., et al. (2019b). High climate sensitivity in the Community Earth System Model Version 2 (CESM2). *Geophysical Research Letters*, 46, 8329– 8337. doi: 10.1029/2019GL083978.

Golaz, J., Larson, V.E., & Cotton, W.R. (2002). A PDF-Based Model for Boundary Layer Clouds. Part I: Method and Model Description. *J. Atmos. Sci.*, *59*, 3540–3551, [https://doi.org/10.1175/1520-0469\(2002\)059<3540:APBMFB>2.0.CO;2](https://doi.org/10.1175/1520-0469(2002)059<3540:APBMFB>2.0.CO;2).

Gregory, J. M., et al. (2004). A new method for diagnosing radiative forcing and climate sensitivity. *Geophys. Res. Lett.*, *31*, L03205.

Hu, A., Meehl, G.A., Han, W., Yin, J., Wu, B., & Kimoto, M. (2013). Influence of continental ice retreat on future global climate, *J. Climate*, *26*, 3087–3111, doi:10.1175/JCLI-D-12-00102.1.

Hurrell, J.W., et al. (2013). The Community Earth System Model: A Framework for Collaborative Research. *Bull. Amer. Meteor. Soc.*, *94*, 1339–1360, <https://doi.org/10.1175/BAMS-D-12-00121.1>.

Kay, J. E., et al. (2015). The Community Earth System Model (CESM) Large Ensemble Project: A community resource for studying climate change in the presence of internal climate variability. *Bull. Am. Meteorol. Soc.*, *96*, 1333–1349, doi:10.1175/BAMS-D-13-00255.1.

Kang, S.M., Deser, C., & Polvani, L.M. (2013). Uncertainty in climate change projections of the Hadley Circulation: The role of internal variability. *J. Climate*, *26*, 7541–7554, DOI: 10.1175/JCLI-D-12-00788.1.

Liu, X., Ma, P.-L., Wang, H., Tilmes, S., Singh, B., Easter, R.C., Ghan, S.J., & Rasch, P.J. (2016). Description and evaluation of a new four-mode version of the Modal Aerosol Module (MAM4) within version 5.3 of the Community Atmosphere Model. *Geoscientific Model Development*, *9*, 505–522, doi:10.5194/gmd-9-505-2016.

Meehl, G.A., et al. (2013). Climate change projections in CESM1(CAM5) compared to CCSM4. *J. Climate*, 26, 6287—6308, doi: 10.1175/JCLI-D-12-00572.1.

Meehl, G.A., et al. (2019a). Effects of model resolution, physics, and coupling on Southern Hemisphere storm tracks in CESM1.3. *Geophys. Res. Lett.*, DOI: 10.1029/2019GL084057.

Meehl, G.A., Senior, C.A., Eyring, V., Flato, G., Lamarque, J.-F., Stouffer, R.J., Taylor, K.E., & Schlund, M. (2019b). Context for interpreting the latest values of equilibrium climate sensitivity and transient climate response from the CMIP6 earth system models, *Science Advances*, submitted.

Neale, R.B., Richter, J.H., Jochum, M. (2008). The Impact of Convection on ENSO: From a Delayed Oscillator to a Series of Events. *J. Climate*, 21, 5904–5924, <https://doi.org/10.1175/2008JCLI2244.1>.

O'Neill, B.C., et al. (2016). The Scenario Model Intercomparison Project (ScenarioMIP) for CMIP6. *Geosci. Model Dev.*, 9, 3461-3482, doi:10.5194/gmd-9-3461-2016.

Zhang, G., & Mcfarlane, N.A. (1995). Sensitivity of climate simulations to the parameterization of cumulus convection in the Canadian Climate Centre general circulation model. *Atmosphere-Ocean*, 33, 407–446, doi:10.1080/07055900.1995.9649539.

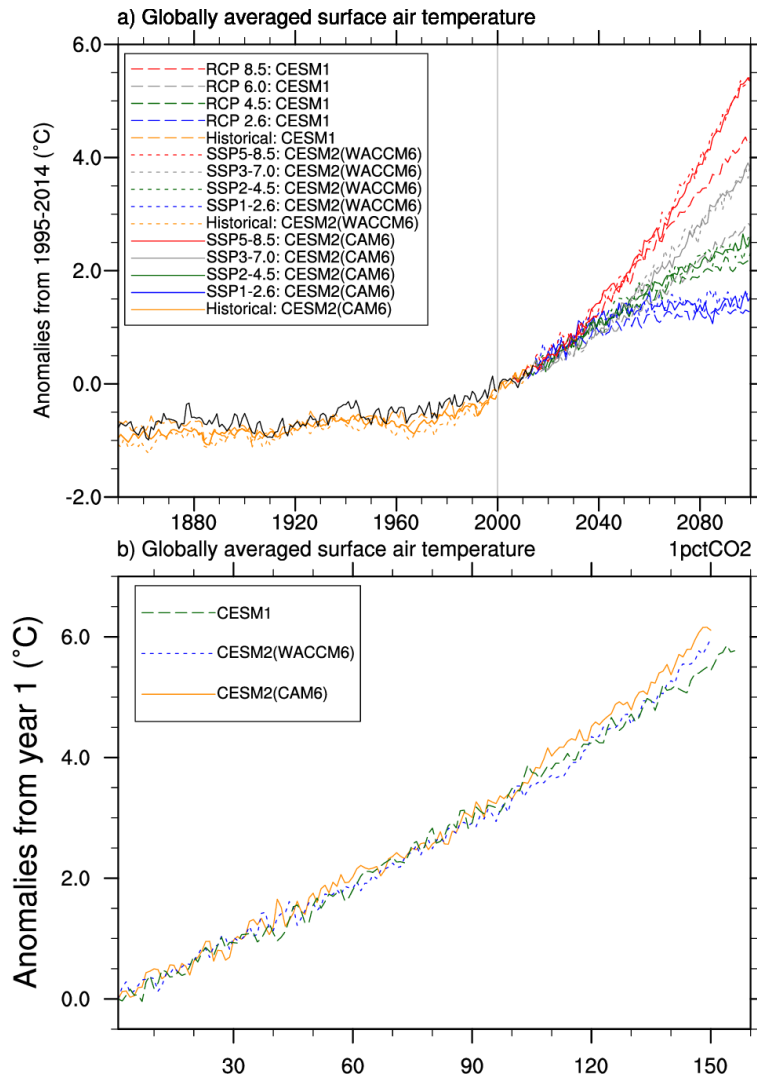


Fig. 1: a) Time series of global mean annual mean surface air temperature anomalies (°C, computed relative to the 1995-2014 base period) for late 19th, 20th and 21st centuries from CESM1, CESM2(CAM6), and CESM2(WACCM6), for the four RCP scenarios for CESM1, and the four SSP scenarios for CESM2(CAM6) and CESM2(WACCM6) as denoted in the text box in the figure; b) same as (a) except for the 1% per year CO₂ increase experiments (°C, anomalies computed relative to each model's first year) where CO₂ doubles around year 70.

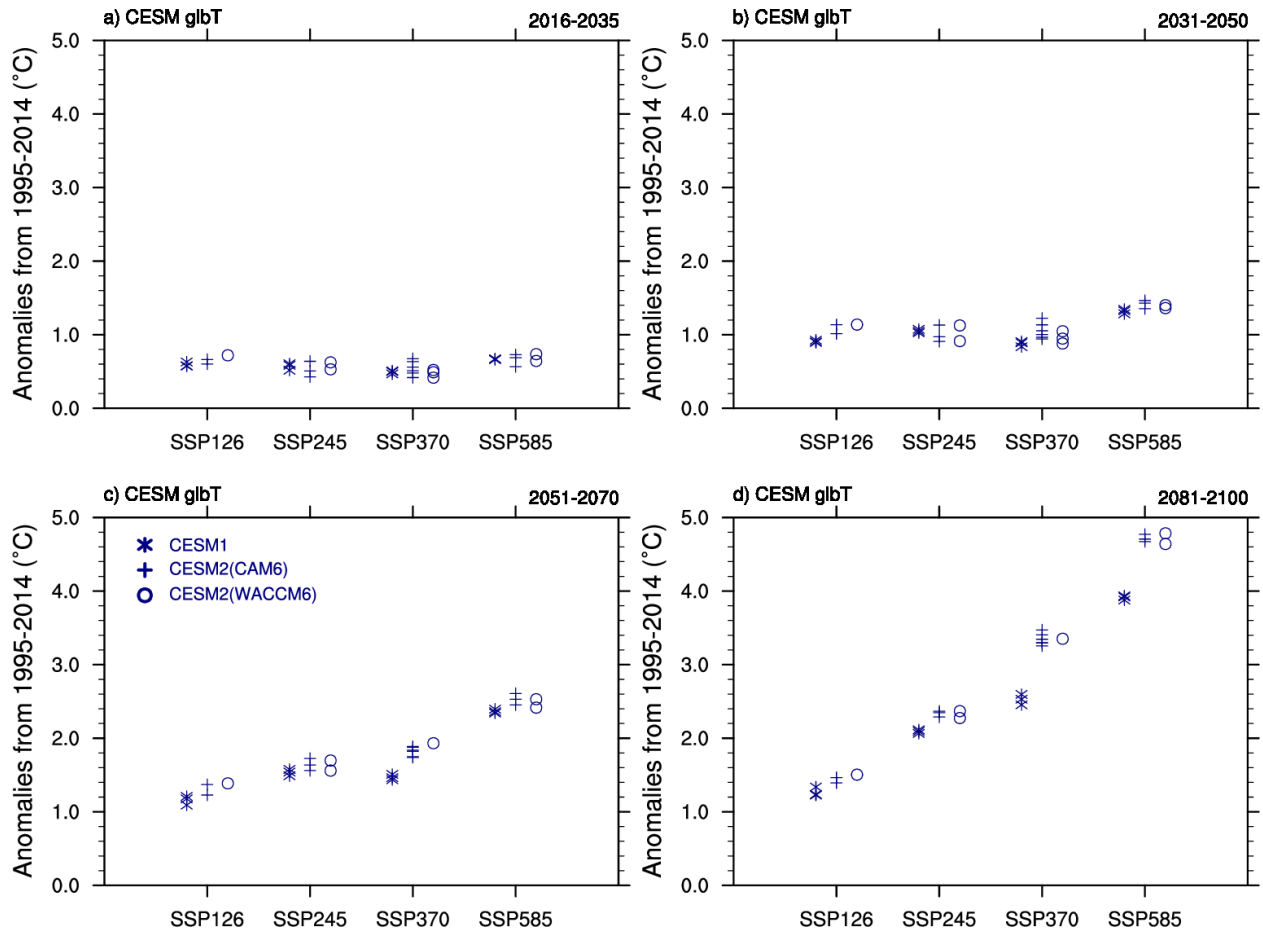


Fig. 2: Globally averaged surface air temperature anomalies (°C, computed relative to the 1995-2014 base period) for the four SSP scenarios and CESM2 models, and comparable RCP scenarios for CESM1 as noted in Fig. 1, denoted in legend in panel (c) with a value plotted for each ensemble member, for a) 2016-2035; b) 2031-2050; c) 2051-2070; and d) 2081-2100.

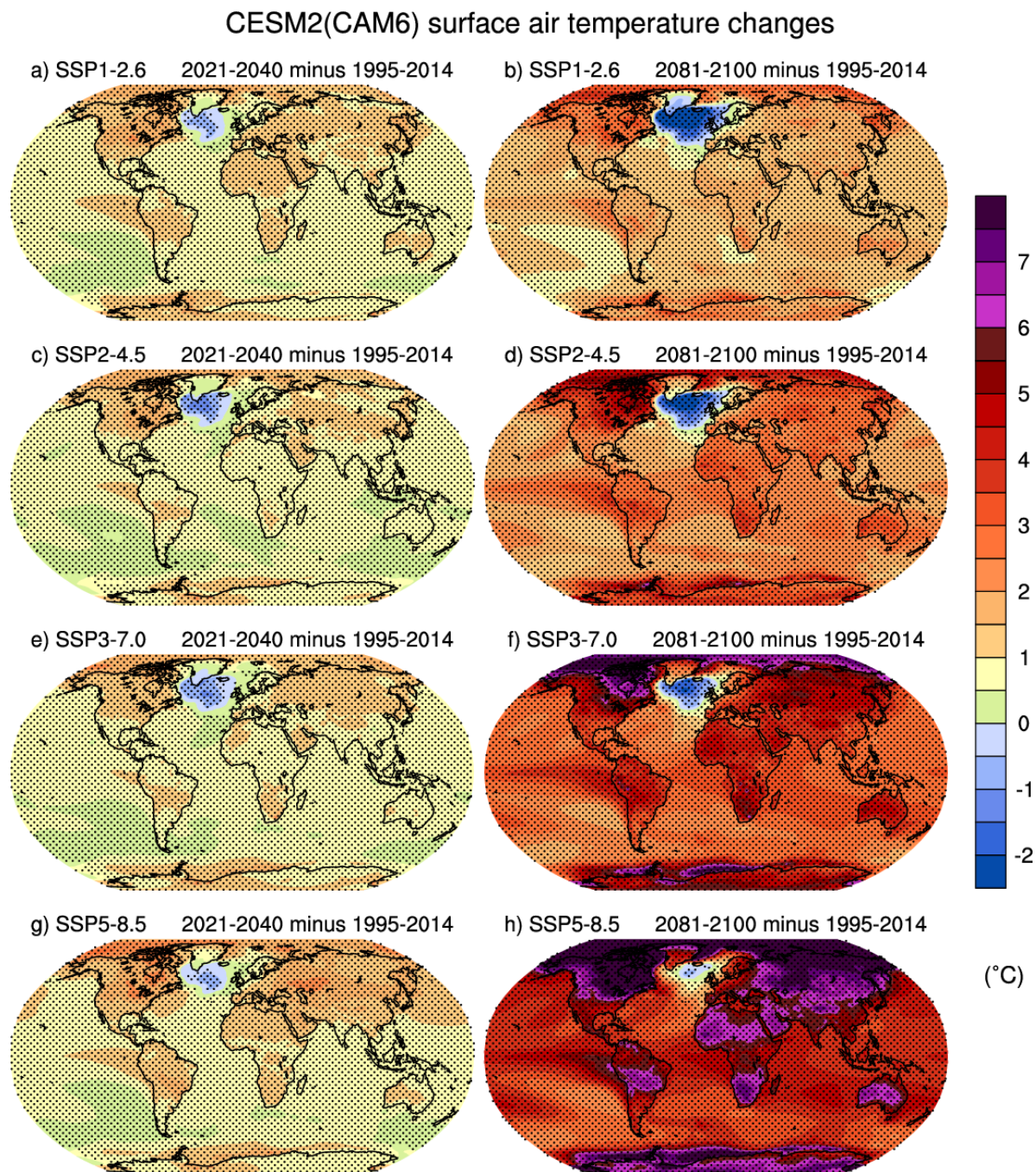


Fig. 3: Surface air temperature anomalies (°C) for CESM2(CAM6) for near-term (2021-2040 minus 1995-2014) (left column), and longer term climate (2081-2100 minus 1995-2014) (right column), for the four SSP scenarios. Stippling indicates statistical significance at the 5% level.

CESM2(WACCM6) surface air temperature changes

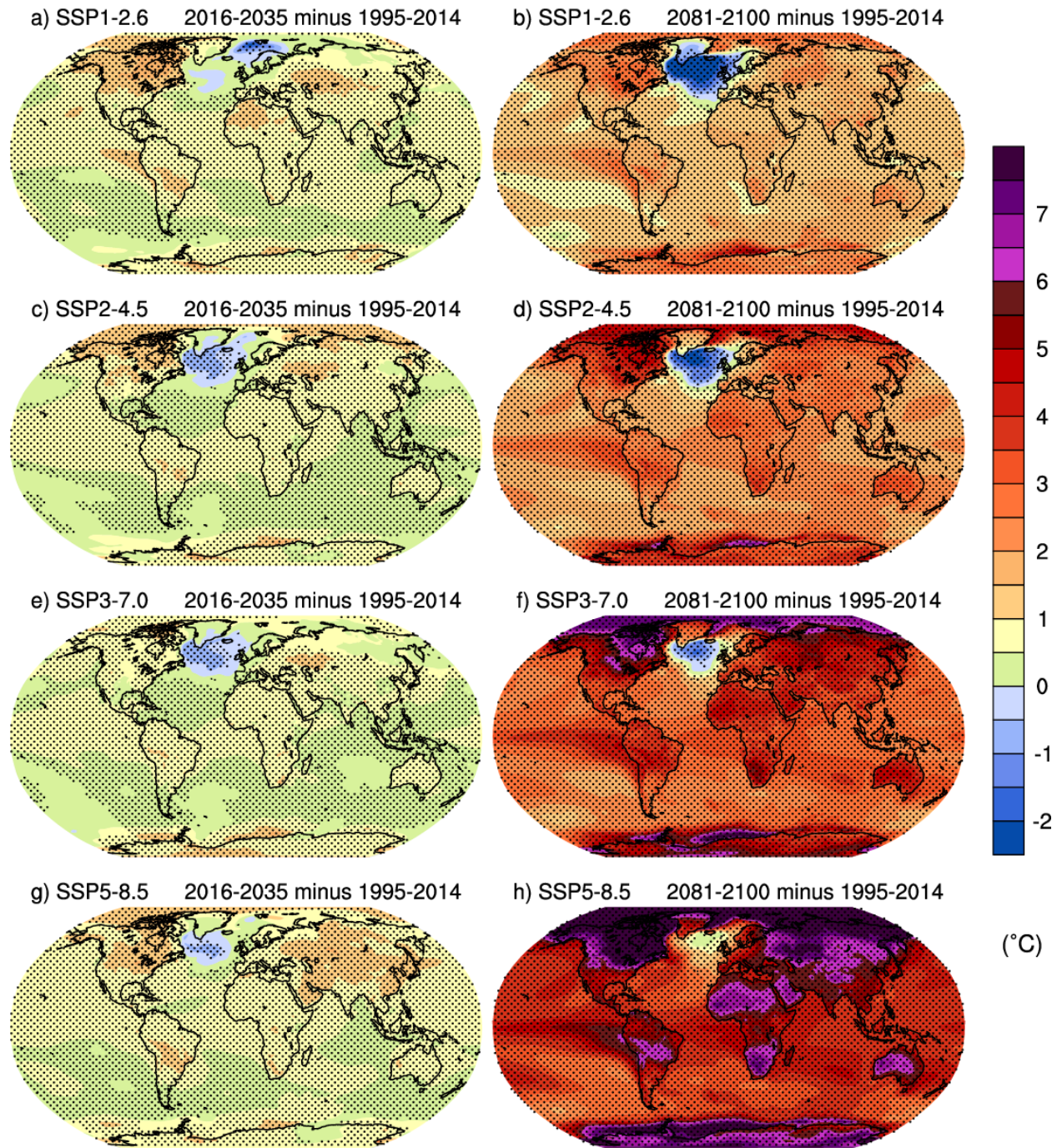


Fig. 4: Same as Fig. 3 except for CESM2(WACCM6).

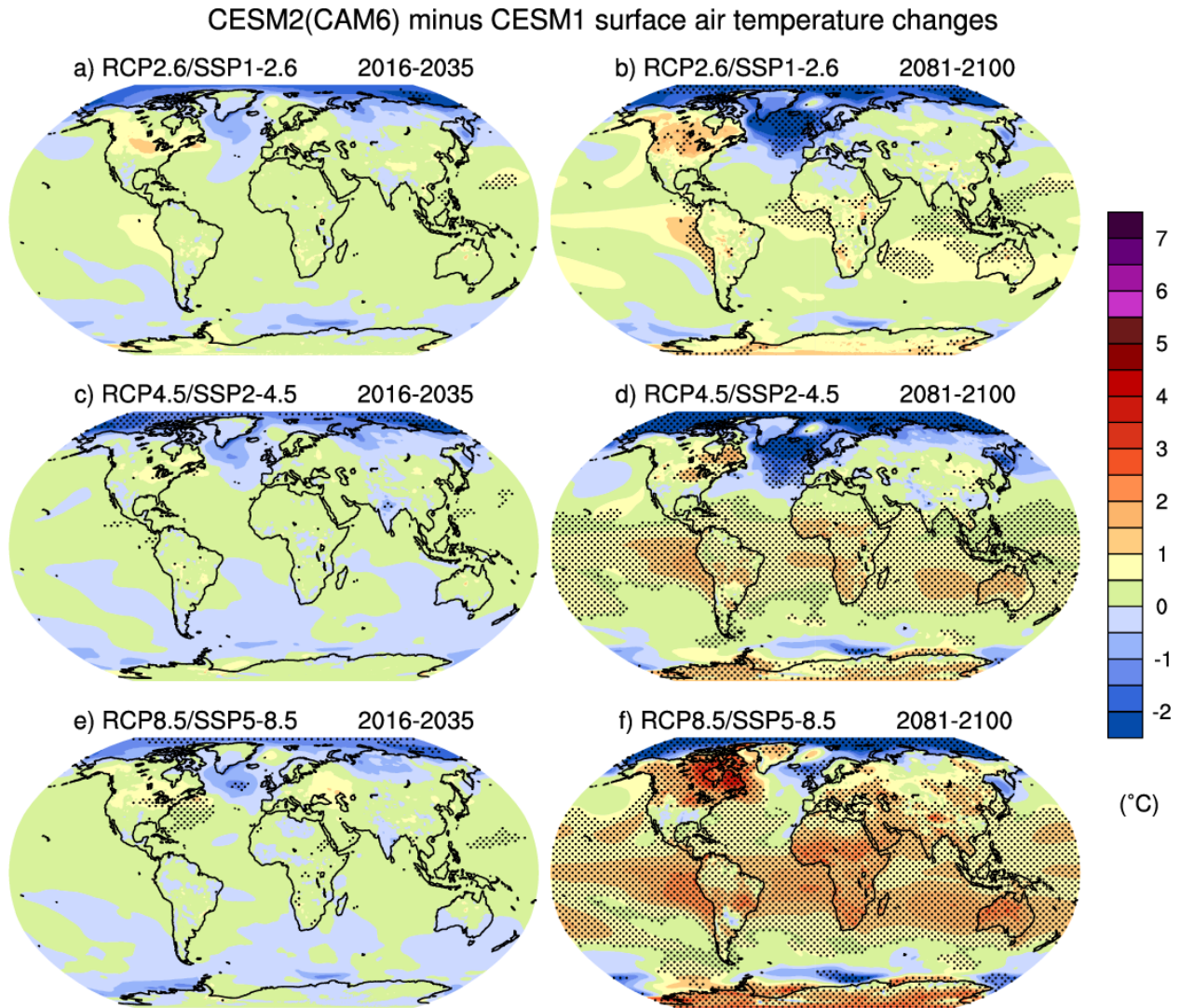


Fig. 5: Same as Fig. 3 except for the differences, CESM2(CAM6) minus CESM1 (SSP3-7.0 and RCP6.0 are not plotted due to the differences in their forcings).

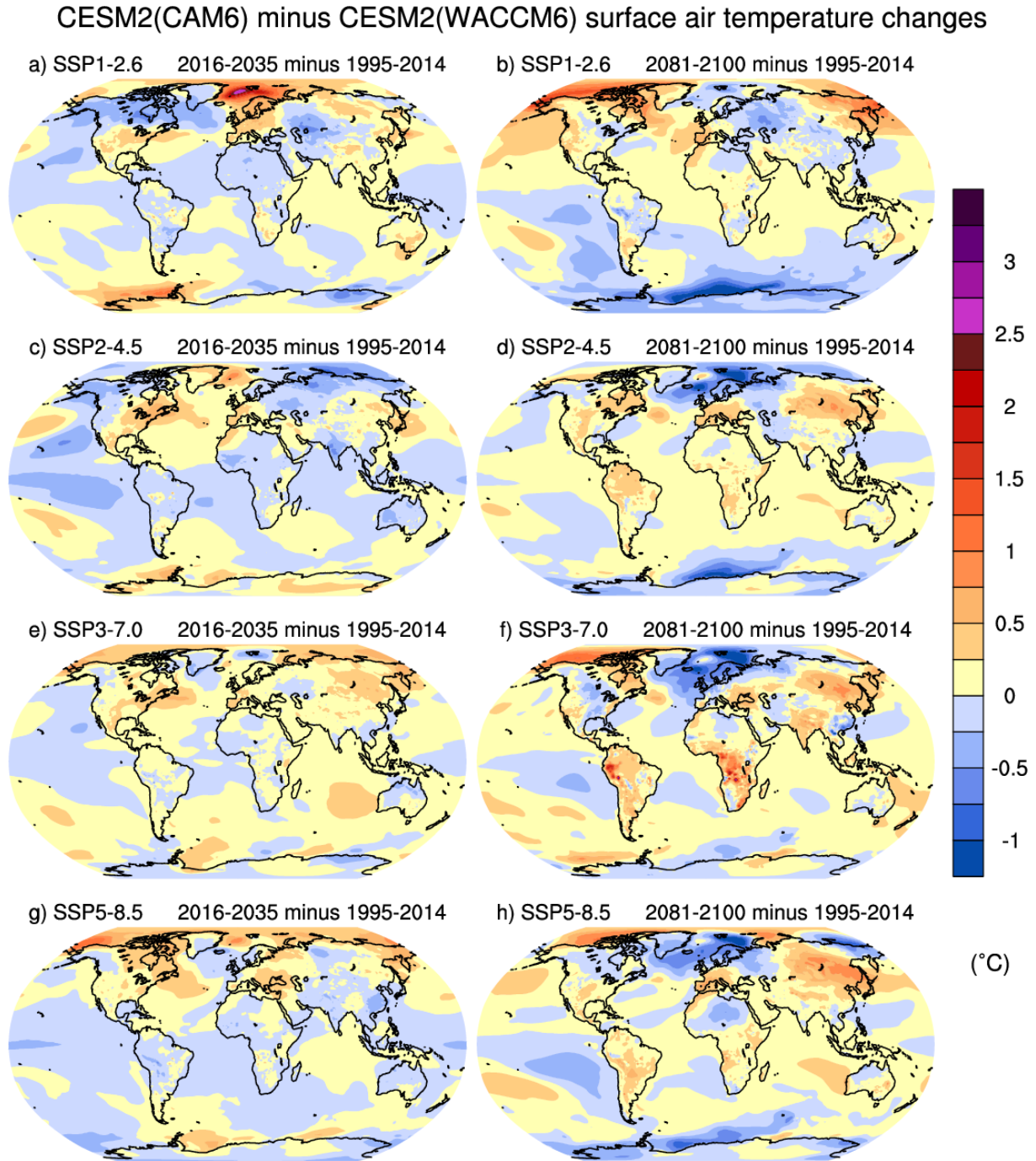


Fig. 6: Same as Fig. 5 except for CESM2(CAM6) minus CESM2(WACCM6) with the addition of SSP3-7.0. No significance is indicated due to the availability of only a single member of CESM2(WACCM6) for some of the scenarios and time periods shown (see Table 1).

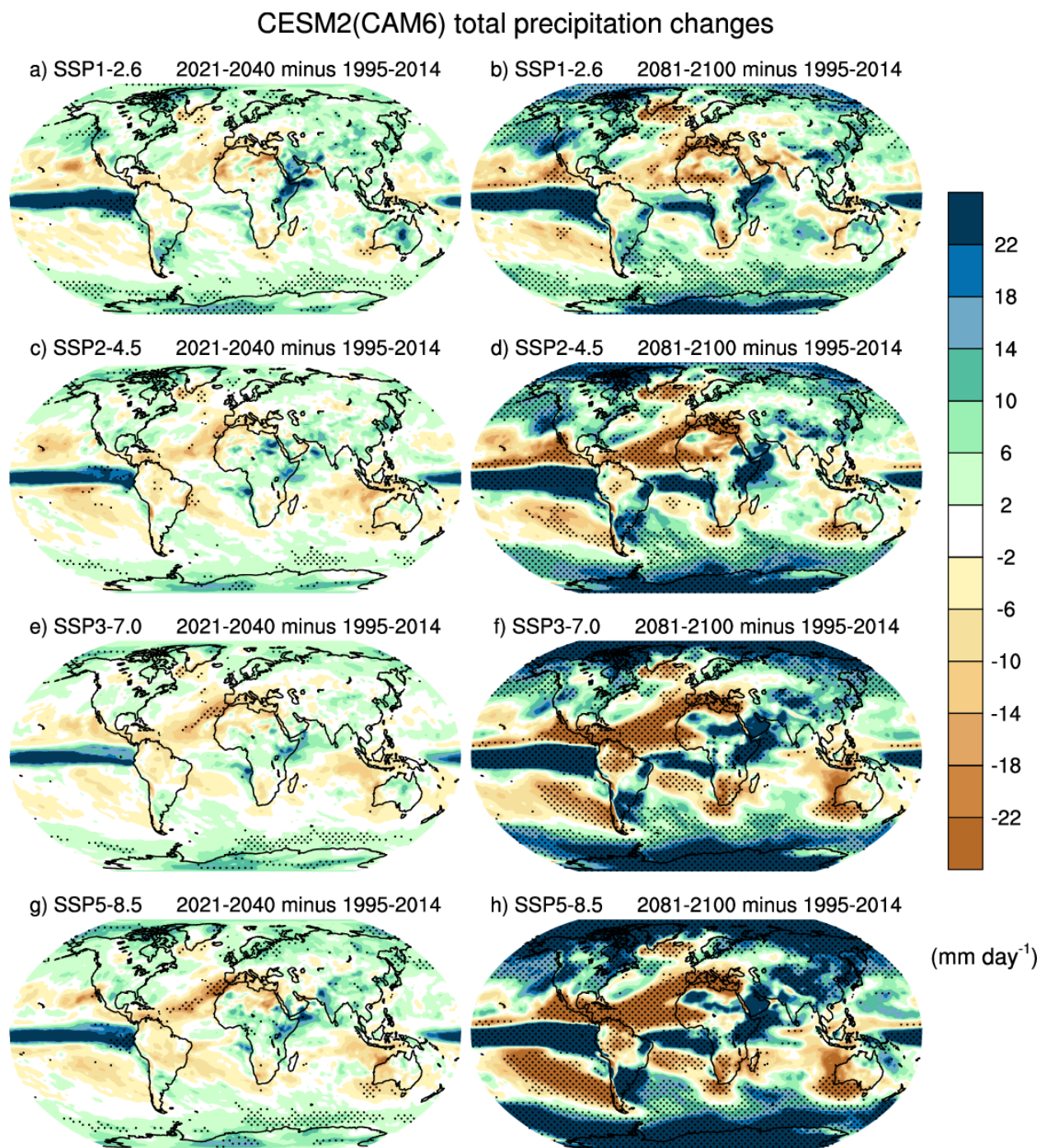


Fig. 7: Same as Fig. 3 except for precipitation (mm/day).

CESM2(WACCM6) total precipitation changes

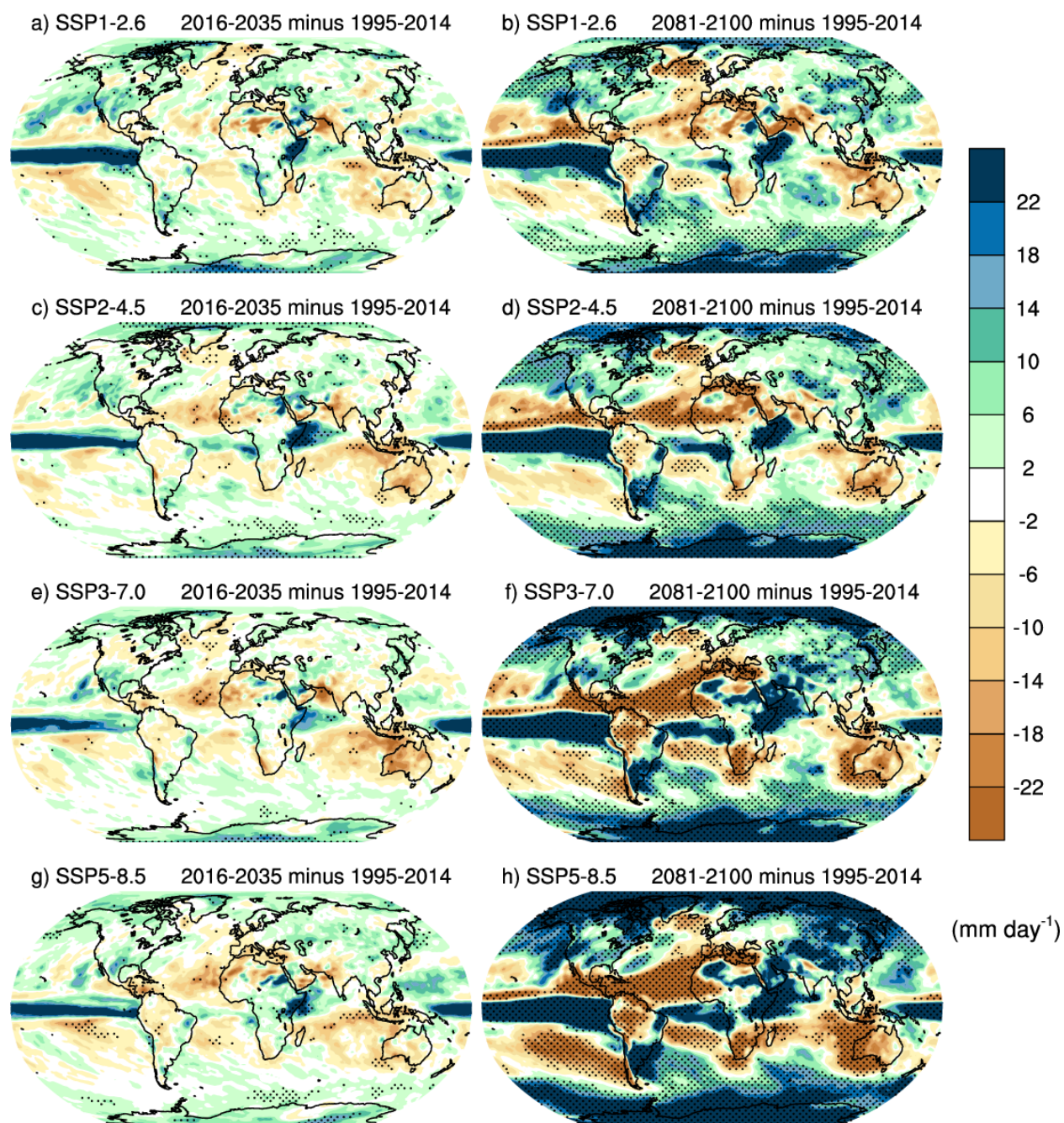


Fig. 8: Same as Fig. 4 except for precipitation (mm/day).

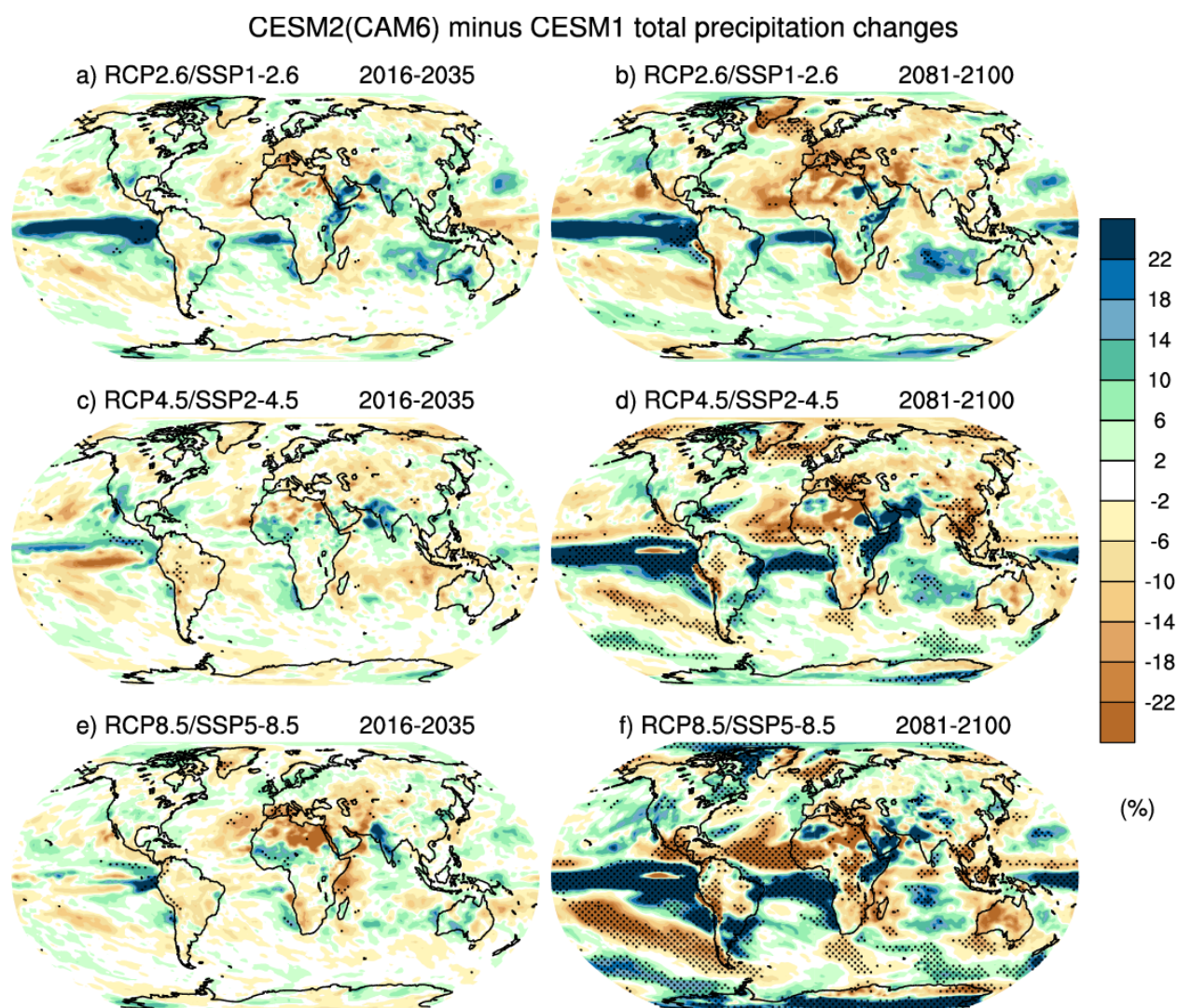


Fig. 9: Same as Fig. 5 except for precipitation (mm/day).

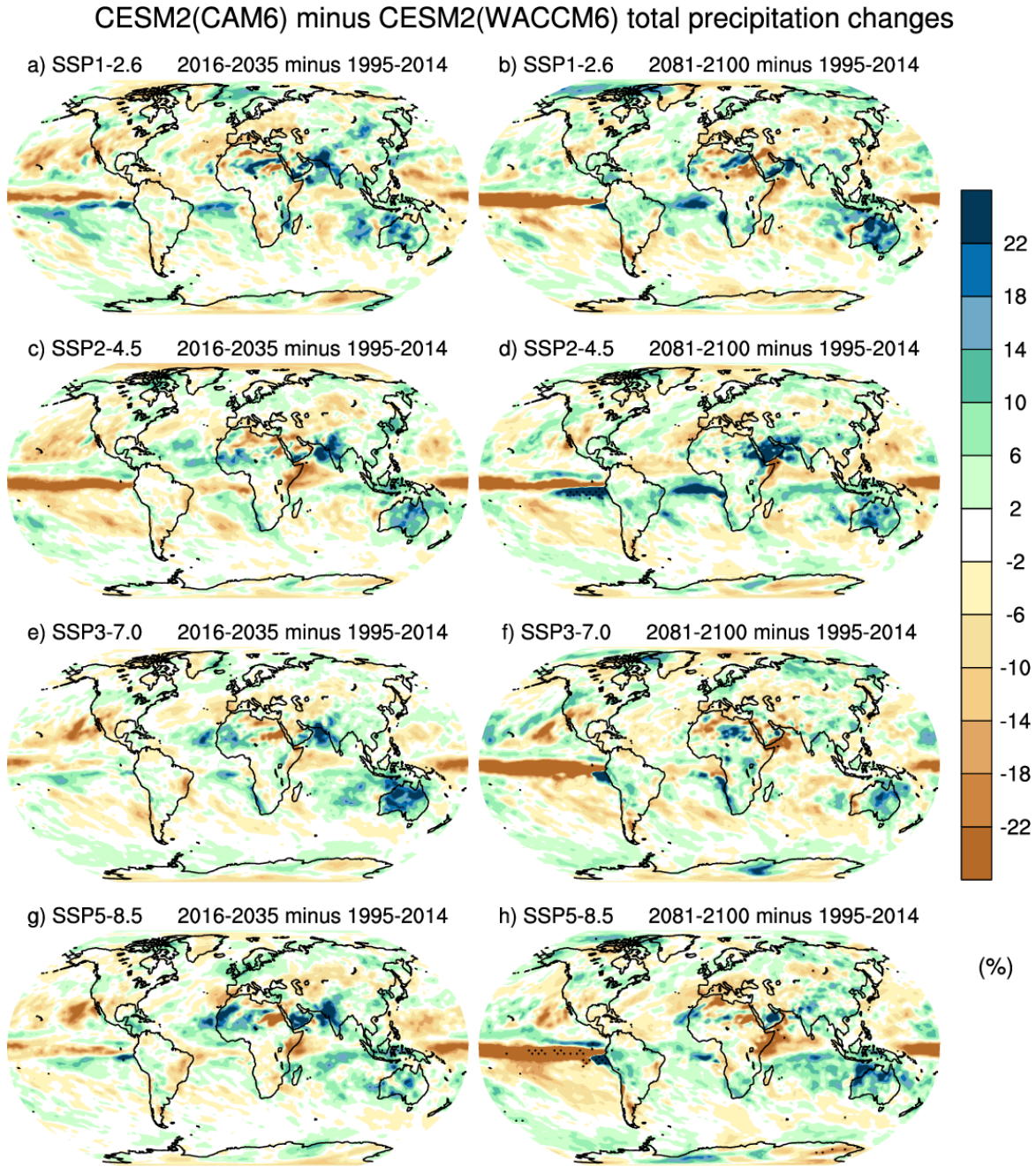


Fig. 10: Same as Fig. 6 except for precipitation (mm/day). No significance is indicated due to the availability of only a single member of CESM2-WACCM for some of the scenarios and time periods shown (see Table 1).

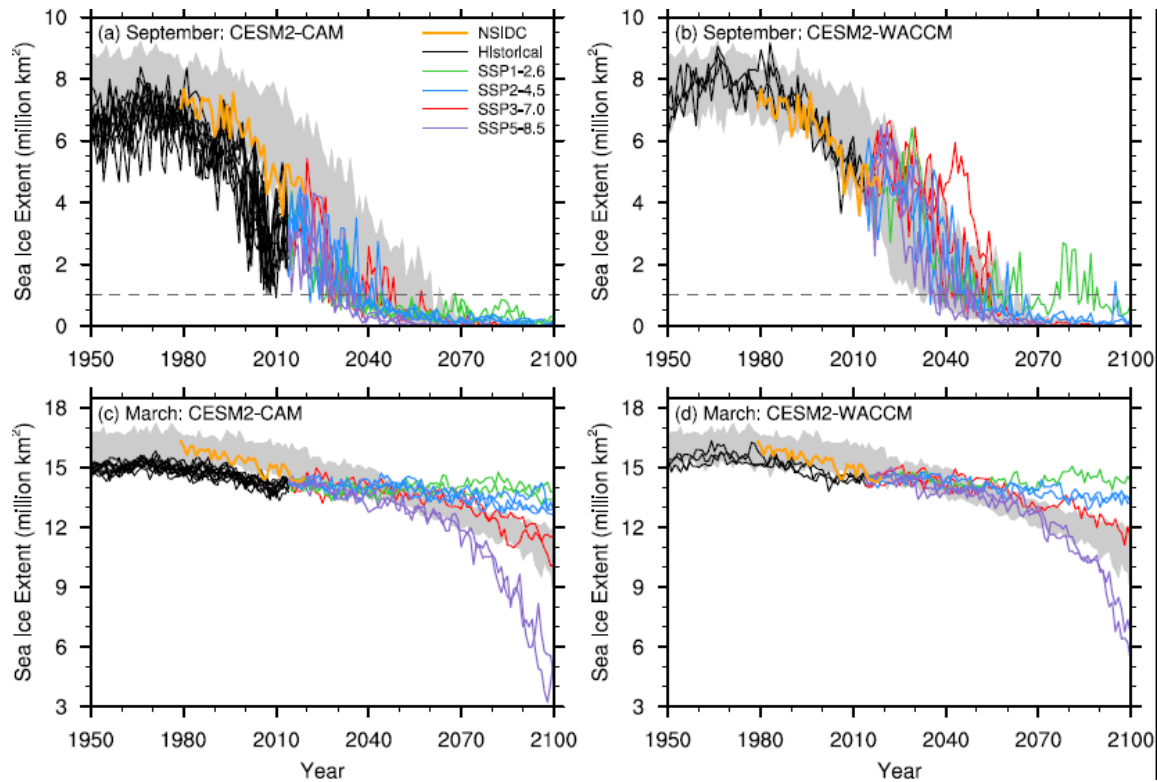


Fig. 11: Time series of Arctic sea ice extent (million km²) over the historical period and for the four scenarios (legend in this panel) compared to the gray shading which represents the range in the CESM1 Large Ensemble, and observations from NSIDC (orange), for a) CESM2(CAM6) denoted CESM2-CAM in figure, September, b) CESM2(WACCM6), denoted CESM2-WACCM in figure, September; c) CESM2(CAM6) March; d) CESM2(WACCM6) March. Dashed lines indicate the threshold for ice-free conditions of less than 1 million km².

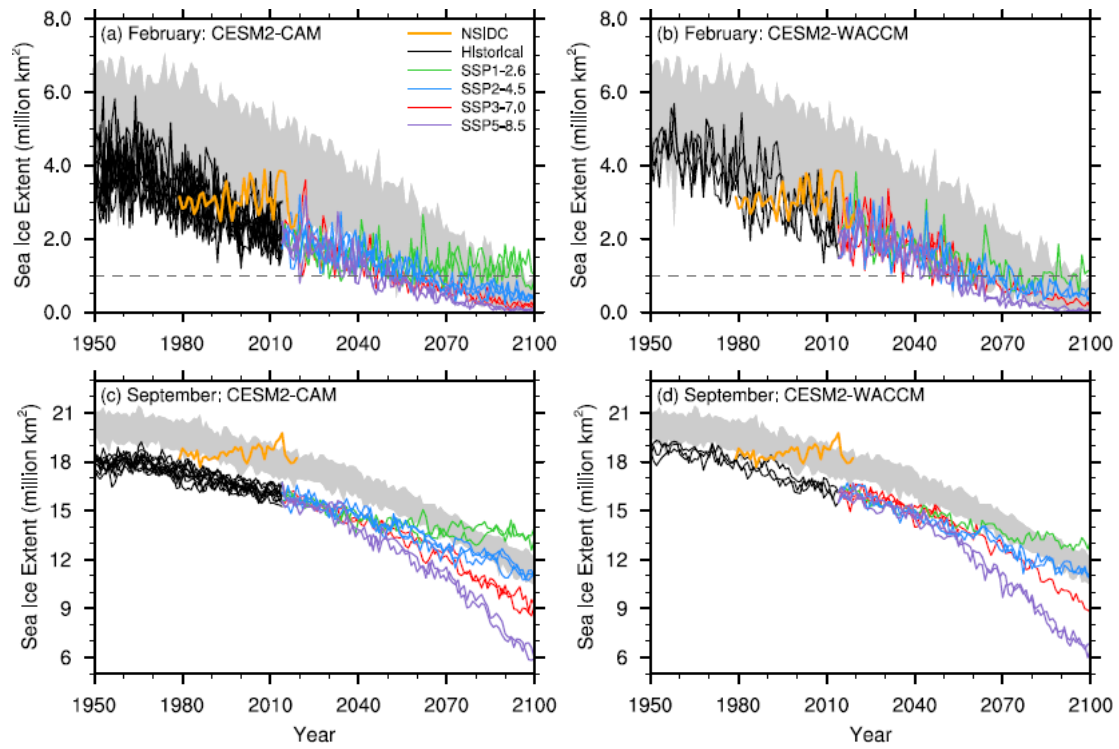


Fig. 12: Same as Fig. 11 except for Antarctic sea ice extent for February (a,b) and September (c,d).